Electron Microscopy Studies of $W_{18}O_{49}$. 2. Defects and Disorder Introduced by Partial Oxidation

WUBESHET SAHLE

Department of Inorganic Chemistry, Arrhenius Laboratory, University of Stockholm, S-106 91 Stockholm, Sweden

$W_{18}O_{49}$ was oxidized in air at about 500K for different intervals of time. Defects of various kinds, related to structures of higher oxides, were observed. These were a coherent intergrowth of $W_{12}O_{34}$, {102}, and {103} crystallographic shear, and WO_3-type structures. A new type of TTB structure was also observed as a defect. Its formation mechanism is proposed and discussed.

Introduction

A preceding paper (*1*) reported observations of planar faults in as-reduced $W_{18}O_{49}$, and stated that the proportion of crystal fragments with these faults did not amount to more than 7% of the total number when the samples had been prepared by gaseous reduction of WO_3 crystals. The observed structure of the defects suggested that they had an oxygen-to-tungsten ratio higher than that of the matrix. In view of the limited information available on the accommodation of defects in $W_{18}O_{49}$, it was considered desirable to examine the microstructure of $W_{18}O_{49}$ crystals that had been deliberately oxidized and to study the accommodation of defects in the host lattice. This would also throw light upon the mechanism of oxidation of the phase.

Experimental

$W_{18}O_{49}$ crystals, prepared in the way described earlier (*2*), were slightly oxidized by placing the samples in a silica tube open to the air at one end and keeping them at about 500K for 1, 7, and 14 days. X-Ray powder diffraction patterns were recorded in a Guinier–Hägg camera, but the main studies were made by means of high-resolution transmission electron microscopy (HREM). The HREM technique employed has been described previously (*1*).

Results

The X-ray powder diffraction patterns of the samples before and after oxidation showed no differences in line positions, which is in accordance with the very limited homogeneity range reported for $W_{18}O_{49}$ (*3, 4*). No extra lines, sharp or diffuse, were observed. On the other hand, the electron diffraction patterns indicated the presence of a few fragments that had been completely transformed to higher oxides by oxidation for 1 or 2 weeks.

Representative micrographs showing the various defects observed in the oxidized crystals are shown in Figs. 1 to 9. The defects will be discussed in order of ascending
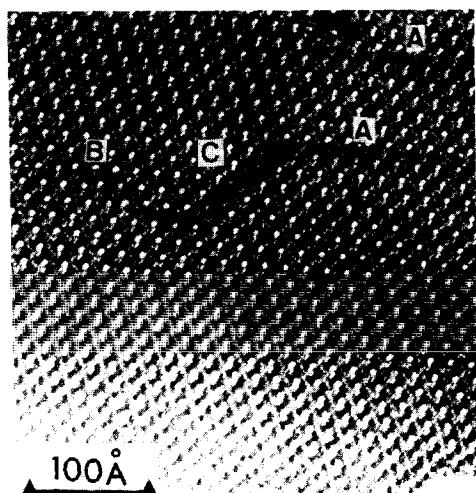
334

FIG. 1. Micrograph of a thin $W_{18}O_{49}$ crystal fragment. Diagonally from upper-left corner runs a $(\bar{2}01)$ defect (labeled B), on the right side of the micrograph are two parallel $(\bar{1}01)$ defects (A), and in the middle a WO_3 network (C) is seen.

degree of oxidation: (i) defects observed also in as-reduced crystals (1), (ii) defects containing a tetragonal tungsten bronze (TTB) -type structure, (iii) those containing crystallographic shear (CS) structures, and (iv) defects composed of the WO_3-type structure.

(i) $(\bar{2}01)$ and $(\bar{1}01)$ Defects

Planar defects along (100), $(\bar{2}01)$, and $(\bar{1}01)$ planes with respect to the host lattice were the only ones likely to affect the local composition that were observed in as-reduced $W_{18}O_{49}$ crystals. They were rarely present, and then mostly as single planar faults. Their structures were interpreted and discussed in a previous paper (1).

Samples oxidized for one day contain $(\bar{2}01)$ and $(\bar{1}01)$ defects quite frequently, and in some cases several faults have been observed in the same fragment, as is illustrated in Figs. 1 and 2. One can note that the $(\bar{1}01)$ defects often terminate within the $W_{18}O_{49}$ crystal and are more frequent than the $(\bar{2}01)$ defects. The micrograph of Fig. 2 shows a repetitive pattern of $(\bar{1}01)$ defects.

(ii) TTB-Type Defects

A type of defect structure that is new in the tungsten–oxygen system was commonly observed in crystals oxidized for 1 week; it is shown in Figs. 3a and b. The resolution in the thin part of this image is quite good, and details of the defect structure can easily be discerned. A reasonable model is presented in Fig. 3c. It consists of a thin slab of TTB-type structure with one-half of the pentagonal tunnels filled to form pentagonal columns (PCs). It can be formed in the regular $W_{18}O_{49}$ structure by splitting PC pairs and introducing a lateral lattice shift across the defect as shown in Fig. 4. This model implies that along the defect the W–W bonds across the edges of the PC pairs have been broken, and the average oxidation state of tungsten has increased by introduction of the necessary extra oxygen atoms. In accord with the micrograph (Fig. 3b), the rows of empty pentagonal tunnels thus formed are inclined at an angle of about 16° to $(100)_{W_{18}O_{49}}$, which is the defect plane. This defect may not be stable in the host, however, as it is occasionally replaced by local areas of WO_3 structure. It
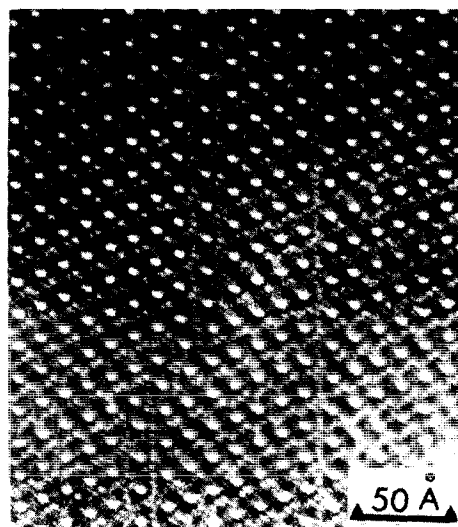

FIG. 2. A micrograph illustrating a repetitive pattern of $(\bar{1}01)$ defects obtained by slight oxidation for 24 hr.
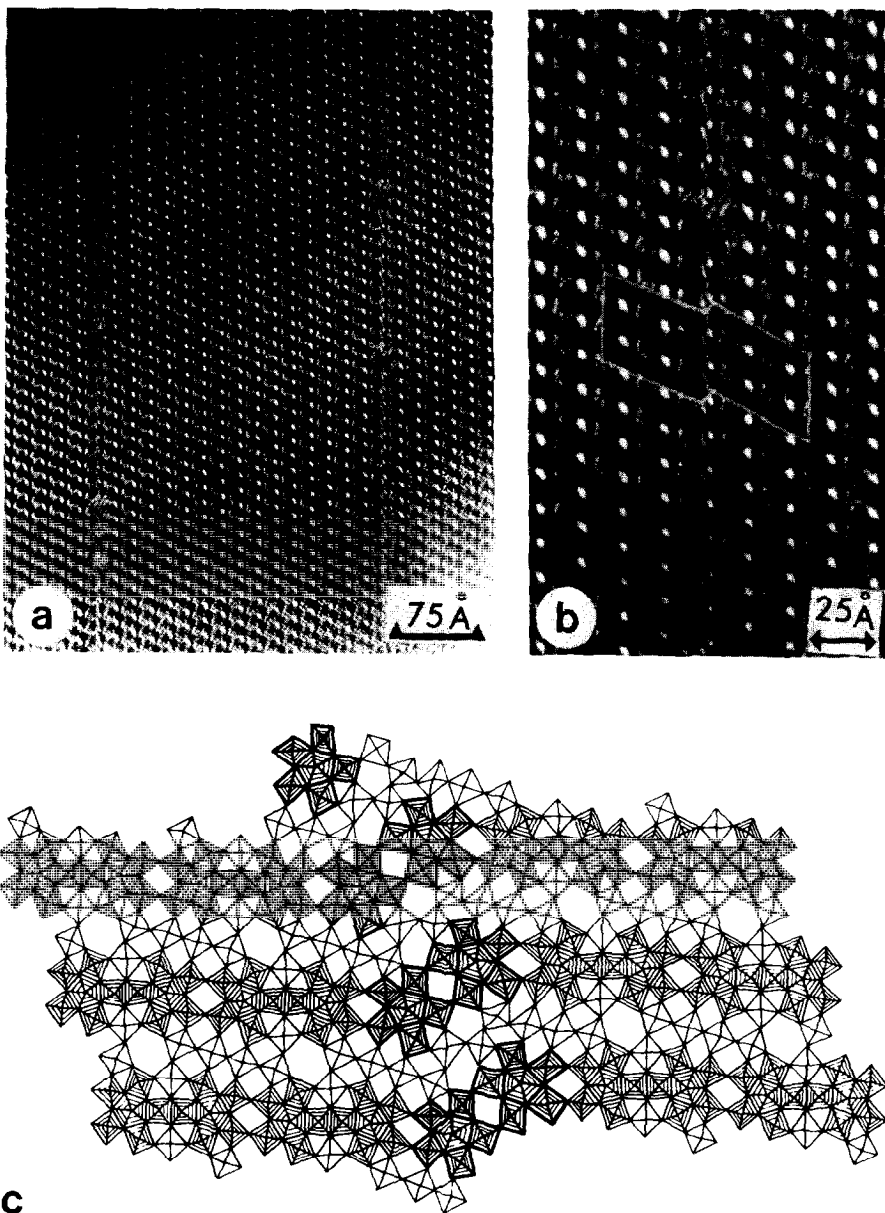
FIG. 3. (a) A TTB-type structure as a new type of structural defect. (b) A portion of (a) at higher magnification. (c) An interpretation of the region within the box in (b).

may thus represent a transitional stage in the formation of a fully oxidized WO_3 structure.

$W_{12}O_{34}$ (5, 6) can be considered as intergrowth of TTB (with half-filled tunnels) and WO_3. Extended areas of $W_{12}O_{34}$ structure

intergrown with $W_{18}O_{49}$ have never been observed, and the transformation from $W_{12}O_{34}$ to $W_{18}O_{49}$ upon reduction proceeds by a nucleation and growth mechanism (2).

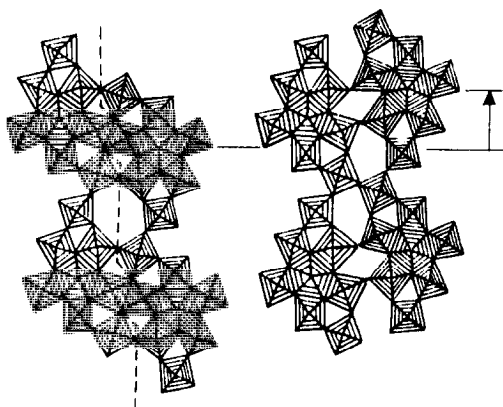Figure 5a shows a wedge-shaped lamellae of predominantly WO_3 grown into

FIG. 4. An illustration of a possible mechanism for the formation of the new TTB-type structural defect in $W_{18}O_{49}$.

$W_{18}O_{49}$. This WO_3 region shows a multitude of contrast features of the same type as previously reported by Iijima and interpreted as TTB-type defects (7). The defect structure enclosed in a box in Fig. 5b can be considered as a microdomain of a homolog of $W_{12}O_{34}$ having wider slabs of WO_3-like structure. Another feature of interest in this micrograph is the misplacement of one hexagonal tunnel at the $W_{18}O_{49}$–WO_3 border, indicated by a thin arrow. An intuitive interpretation of this part is given in Fig. 5c; it implies that a PC–HT–PC unit (8) has formed in twin orientation to those occurring in regular $W_{18}O_{49}$.

(iii) Crystallographic Shear (CS) Structure

An image of a fragment from a sample oxidized for 1 week is presented in Fig. 6. It shows a mixture of three coherently intergrown structures. These are $W_{18}O_{49}$, {103}, and {102} CS, as is best seen in Fig. 6b. The micrograph seems to show a frozen-in stage of a solid-state reaction. Three twin directions of {103} CS are observed, and the CS planes are oriented parallel to (101), ($\overline{6}$01), and ($\overline{3}$02) of the parent ($W_{18}O_{49}$) lattice. As

is indicated in Fig. 6b, the {102} CS structure, which should represent the highest degree of oxidation, is seen to be interleaved between the lower oxides in this projection.

(iv) WO_3 Structure Type

Extended defects of WO_3 structure type were observed in the samples oxidized for 1 and 2 weeks, but not in the samples oxidized for only 1 day. A low-magnification micrograph of a defective $W_{18}O_{49}$ fragment is shown in Fig. 7. Strips of various widths of WO_3 structure are lined up parallel to the (100) plane of $W_{18}O_{49}$ and could be designated as (100)–WO_3 defects. The rows of pseudohexagonal tunnels typical of $W_{18}O_{49}$ extend to various lengths into the WO_3 areas, as seen in Fig. 7. At the upper-right corner of the micrograph a twinned part is also revealed.

As can be seen in Fig. 8, the WO_3 structure can be connected in a natural and continuous way to the basic $W_{18}O_{49}$ structure. An interpretation of the thin part is proposed in Fig. 8b. It is likely that such slabs of WO_3 structure can be incorporated in $W_{18}O_{49}$ without causing much distortion. However, an ordered lamellar intergrowth of the two structure types has not been observed. Instead, irregularly shaped areas of WO_3 structure, like that shown in Fig. 9, occur frequently.

Discussion

The purpose of this study was an investigation of the ability of $W_{18}O_{49}$ to accommodate defects and analysis of the structural changes that accompany a slight oxidation of the phase. In all samples the unoxidized $W_{18}O_{49}$ structure remained the predominant part, as indicated by the X-ray powder patterns as well as the electron optical results. Different structures were seen coexisting with this parent phase, and these are likely
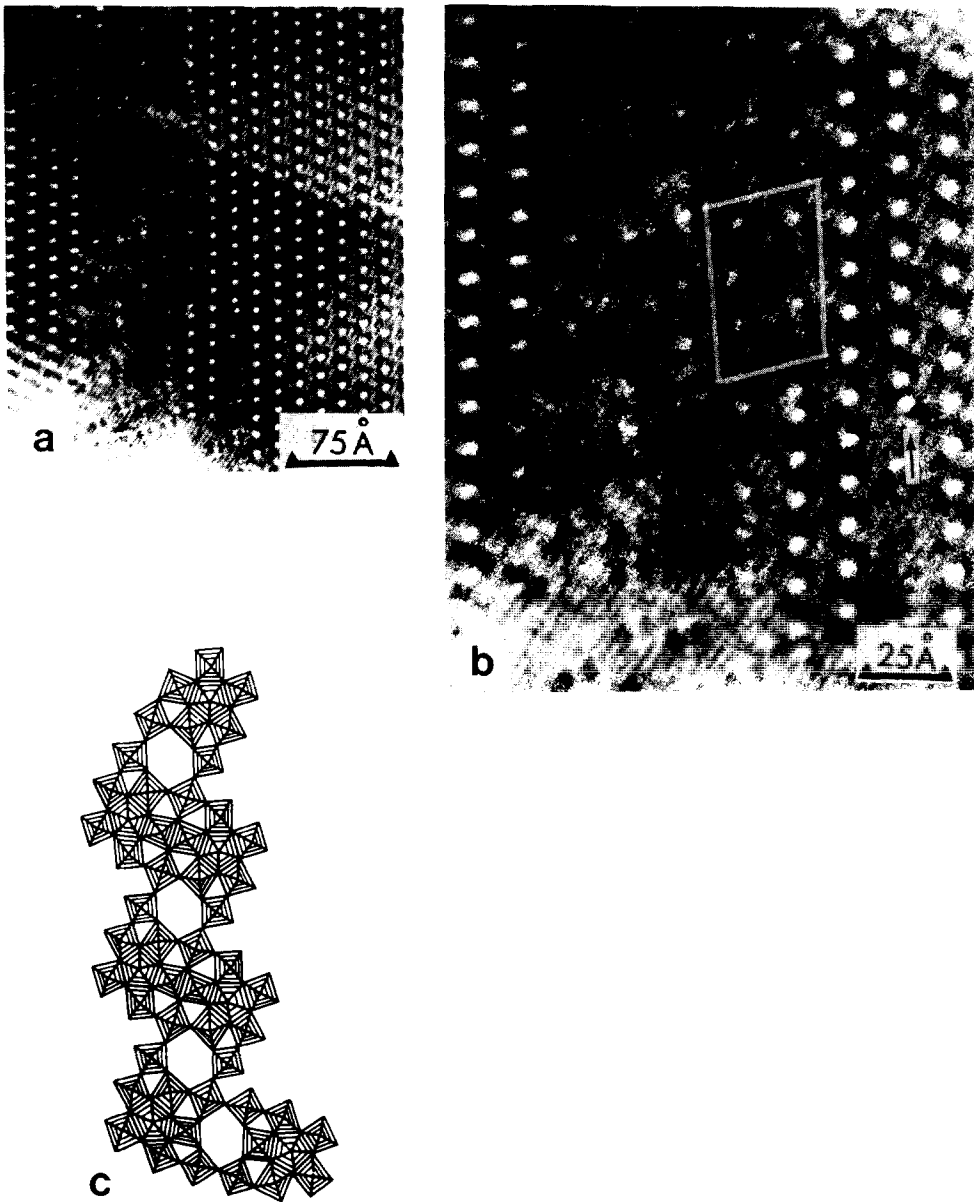
FIG. 5. (a) Micrograph of a thin crystal fragment showing microdomains of $W_{12}O_{34}$ homolog and WO_3 structures within the $W_{18}O_{49}$ lattice. (b) Enlargement of the central region of (a). (c) An interpretation of the contrast indicated by a thin arrow in (b).

to represent different stages in the course of oxidation. Unfortunately, it is difficult to reach a definite conclusion concerning the reaction path from the present experiments. The fragments observed in the mi-croscope represent small pieces of the original crystals, and it is impossible to tell from what depth beneath the surface a particular fragment originates.

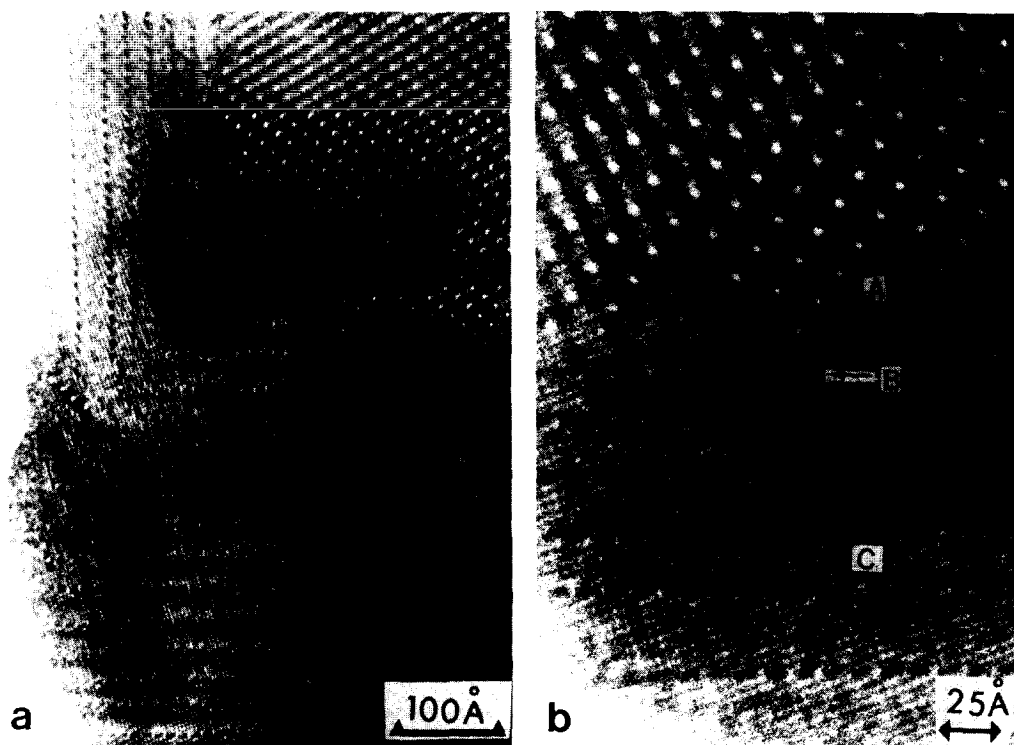A first guess could be that the oxidation

FIG. 6. (a,b) A micrograph of a crystal fragment containing $W_{18}O_{49}$ (A), {102}, and {103} CS structures (B and C, respectively).

proceeds as a reversal of the reduction. The sequence of phases formed upon reduction at about 1270K is $WO_3 \rightarrow$ {102}–$CS \rightarrow$ {103}–$CS \rightarrow W_{12}O_{34} \rightarrow W_{18}O_{49}$ (2). It is not
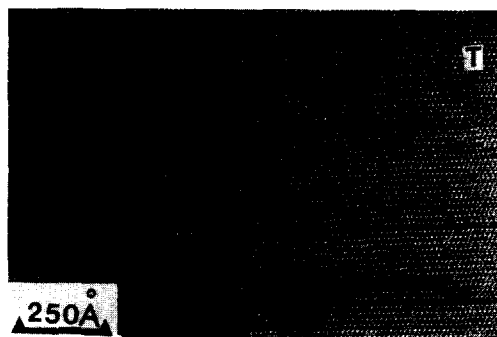

FIG. 7. A low-magnification electron micrograph of a defective $W_{18}O_{49}$ crystal fragment. Stripes of WO_3-type structure of varying width and length occur parallel to (100) of the host structure. A twin region (upper-right corner of the micrograph, T) is also seen.

certain, however, that all these phases would form at lower temperatures. At least small areas of all the higher oxide phases and sometimes totally transformed fragments were observed in the present studies.

The defects observed can be considered as local intergrowths of other structure types in $W_{18}O_{49}$. In only two cases has clustering of defects been observed, viz., three (10$\bar{1}$) defects as seen in Fig. 2 and four (100) TTB-type defects; part of the cluster is shown in Fig. 3a. Since no further repetition was observed, these intergrowth structures are probably formed by chance and are not thermodynamically particularly favorable.

The most probable first oxidation step of the phase, however, is the breaking of the Me–Me bond at the edge-shared PC pairs, which requires extra oxygen. This process
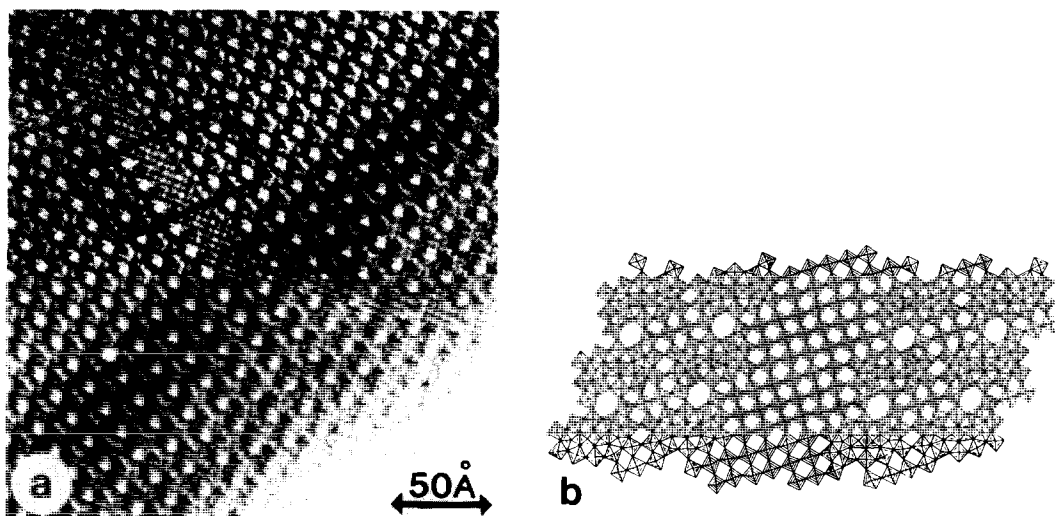
FIG. 8. (a) A micrograph of a crystal fragment containing a rarely observed type of WO_3 microdomain of uniform width. (b) An interpretation of the microstructure enclosed in (a).

may result in the formation of either of three of the unrelated defect types: (i) the $(\bar{2}01)$ defect, (ii) the $(\bar{1}01)$ defect, or (iii) the (100) TTB defect. The existence of these microstructures suggests that a slight oxidation directly yields one of these alternative reaction products.

The further path cannot be traced in detail, but the structural relation between the transformed areas and the parent structure shows that the oxidation is a coherent process. It is, however, easy to imagine a mechanism whereby the (100) TTB defect is transformed into the (100)–WO_3 defect, as the micrograph of Fig. 3 suggests.

The CS structures topotactically intergrown with $W_{18}O_{49}$ (Fig. 6) are more difficult to explain. They could be formed either by oxidation of (100) TTB or could result from reduction of a domain previously oxidized to WO_3. Such reduction could occur by the action of the electron beam and the vacuum of the microscope. This could be true for the {102} CS element indicated in Fig. 6b, but the {103} CS planes are unlikely to have been formed in the microscope.

The first diffraction pattern taken of the fragment with a defocused beam indicated the presence of the CS phases, and no change in the pattern was observed by subsequent irradiation even with a focused beam. Moreover, CS planes grown by beam heating are generally not perfectly straight, as they contain local segments of other types of shear structures (6, 9, 10). This is not the case here, and another and more probable alternative is that a local and temporary re-reduction may have taken place during the preparation heat treatment as a secondary reaction. This could be because the diffusion of oxygen from the surface was hindered or slowed. It is probable that the rather wide pseudohexagonal tunnels in $W_{18}O_{49}$ are important for the transport of oxygen into the structure as long as they are available.

Further experiments are obviously required in order to give a full understanding of this process. This study shows, however, that at low temperature the reoxidation of $W_{18}O_{49}$ proceeds, at least initially, by a coherent transformation mechanism.
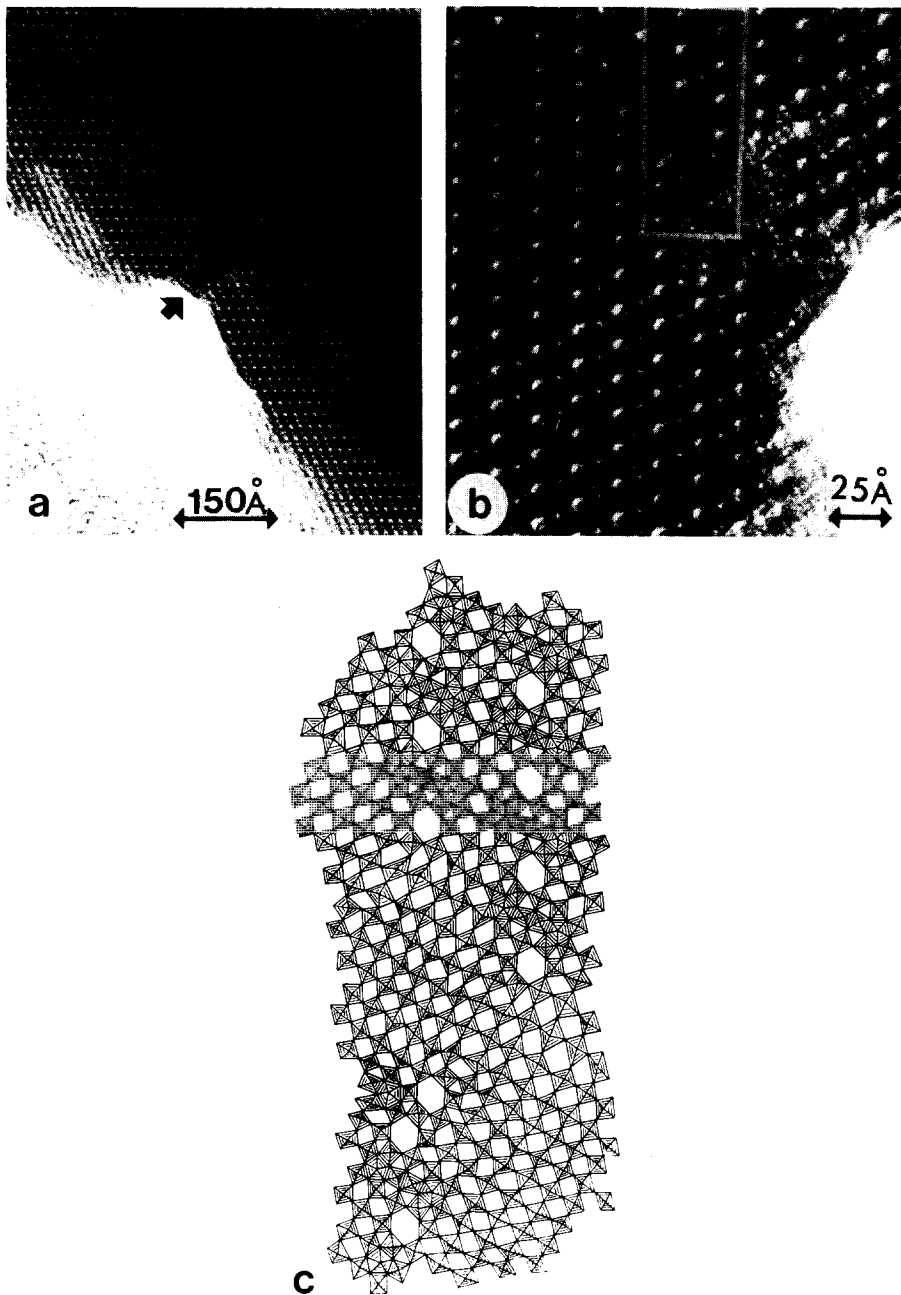
FIG. 9. (a) Electron micrograph showing a wider view of a representative fragment in which there is regional distruction of the $W_{18}O_{49}$ lattice due to slight oxidation. (b) Enlargement of the defective region in (a) indicated by an arrow. (c) An interpretation of the enclosed region of (b).

Acknowledgments

References

1. W. SAHLE, *J. Solid State Chem.* **45,** 324 (1982), and references therein.

2. S. BERGLUND AND W. SAHLE, *J. Solid State Chem.* **36,** 66 (1981).

3. J. F. MARUCCO, P. GERDANIAN, AND M. DODE, *J. Chim. Phys.* **66,** 674 (1969).

4. T. EKSTRÖM, *Chem. Commun. Univ. Stockholm,* No. 7 (1975).

5. M. SUNDBERG, *Chem. Scr.* **14,** 161 (1978–79).

6. M. SUNDBERG, *Chem. Commun. Univ. Stockholm,* No. 5 (1981).

7. S. Iijima, *Acta Crystallogr. Sect. A* **34,** 922 (1978).

8. W. SAHLE AND M. SUNDBERG, *Chem. Scr.* **16,** 163 (1980).

9. M. SUNDBERG AND R. J. D. TILLEY, *Phys. Status Solidi (A)* **22,** 677 (1974).

10. W. SAHLE, unpublished results.